Analysis of interactive effects of DEM resolution and basin subdivision level on runoff simulation in Kaidu River Basin, China

J. Sun, Y. P. Li, G. H. Huang and C. X. Wang

ABSTRACT

Uncertainties in spatial data associated with basin topography, drainage networks, and land cover characteristics may affect the performance of runoff simulation. Such uncertainties are mainly derived from selection of digital elevation model (DEM) resolution and basin subdivision level. This study focuses on assessing the effects of DEM resolution and basin subdivision level on runoff simulation with a semi-distributed land use-based runoff process model. Twenty-four scenarios based on various DEM resolutions and subdivision levels are analyzed for the Kaidu River Basin. Results can be used for quantifying the uncertainty of input data about spatial information on model simulation, disclosing the interaction between DEM resolution and subdivision level, as well as identifying the optimal system inputs. Results show that the model performance could be enhanced with the increased subdivision level. Results also reveal that the interaction of DEM resolution and subdivision level has slight effects on modeling outputs. Multi-objective fuzzy evaluation is used to further examine the uncertainty in DEM resolution and basin subdivision level on model performance. The results indicate an optimal combination of input parameters is suitable for Kaidu River Basin which could lead to more reliable results of the hydrological simulation.

Key words | basin subdivision, DEM, hydrological modeling, interaction analysis, SLURP, uncertainty

J. Sun
C. X. Wang
Sino-Canada Resources and Environmental Research Academy,
North China Electric Power University,
Beijing 102206,
China

Y. P. Li (corresponding author)
G. H. Huang
School of Environment,
Beijing Normal University,
Beijing 100875,
China
E-mail: *yongping.li@iseis.org*

INTRODUCTION

Uncertainties in spatial data associated with basin topography, drainage network, and land cover characteristics may affect the performance of runoff simulation in hydrological models (Du *et al.* 2009; Li *et al.* 2014; Tan *et al.* 2015). Spatial data in a given basin are usually estimated by digital elevation models (DEMs). However, DEM resolution, as well as the number and the manner of subdividing a basin can impact the quality of spatial data (Pradhanang & Briggs 2014; Yan & Zhang 2014). The quantification of the uncertainty in the spatial input data associated with DEM resolution and basin subdivision levels could lead to producing more reliable results from models' calibration and simulation processes (Xu 1999; Li & Xu 2014).

DEM is useful for providing necessary input to hydrological models and convenient for representing the continuously varying topographic surface of the earth (Ma 2014; Blanchard *et al.* 2015). Different DEM resolutions may result in different topographical variations, such as elevation and slope. Singh *et al.* (2015) indicated that the topographical variations in terms of elevation differences can bring significant changes in the corresponding basin parameters and resultant runoff processes. The effects of DEM resolutions on hydrological simulation have attracted the attention of many researchers. Yu (1997) set a series of DEMs (varying from 37 m to 1,097 m resolution) for examining DEM resolution effects on hydrological simulation via the basin scale hydrologic model for a basin of 1,437 km^2; the study suggested that 183 m resolution could be an appropriate selection in terms of the quality of hydrologic simulation and the amount of required computing

doi: 10.2166/nh.2016.332

time. Wu *et al.* (2007) adopted 12 resolutions of DEMs (ranging from 30 m to 3,000 m) for hydrological simulation by topography-based rainfall–runoff model (TOPMODEL), and results revealed that decreasing DEM resolution would deteriorate topographic index distributions and model simulation; moreover, the basin size does play an important role in the resolution dependency of TOPMODEL. Zhang *et al.* (2014) examined the effects of DEM resolutions ranging from 30 m to 1,000 m on hydrological simulation by the Soil and Water Assessment Tool (SWAT) for a basin of 2,995 km^2, which found that runoff is essentially unaffected by the DEM resolutions and resolution higher than 200 m is the optimal DEM resolution for runoff simulation considering the temporal distribution uncertainties. Generally, the aforementioned studies revealed that DEM resolutions have significant influence on basin delineation and hydrological simulation; however, the finest resolution could not always produce the best simulation results. Particularly for large-scale river basins, due to the complexity of model construct and limitation of data availability, it remains a challenge to select appropriate DEM resolution for hydrological simulation. Therefore, these studies are effective for investigating the effects of DEM resolution on hydrological models.

Subdividing a basin into smaller basic units is also a preliminary and important work for semi-distributed and distributed hydrological models (Xu & Singh 2004; Pradhananang & Briggs 2014). The heterogeneity within the basin and corresponding hydrological processes can be affected by the size and the number of basic units. In recent years, a number of research works have been conducted to explore the effects of basin subdivision level on hydrological simulations. Tripathi *et al.* (2006) compared the simulated water balance components among different basin subdivision levels using the SWAT; results revealed that a marked variation in individual components of water balance is observed under different subdivision levels. Using the SWAT model, Rouhani *et al.* (2009) studied the variation in slow flow and extreme flow simulation due to different basin subdivision levels, which revealed that varying the number of sub-basins can affect the daily total flow component, but the model efficiency is less affected by the variation in basin subdivisions. Han *et al.* (2014) obtained the results of the difference in model efficiency becoming negligible among fine subdivision levels through examining different levels of basin subdivision. Summarily, detailed subdivision levels could provide detailed information about basins; the difference in model performance is slight among different subdivision levels in basins with small size and flat terrain. Therefore, it is interesting to explore whether similar results may be obtained for a large-scale basin with rough terrain and sparse distribution of gauge stations.

The previous studies mainly focused on the effects of DEM resolution or basin subdivision level on hydrological simulation, respectively. However, Kalin *et al.* (2003) found that when the study area is low-relief at different elevations, the basin delineation can be simple; on the contrary, when the area is abrupt, the number of sub-basins would increase to clearly delineate the actual basin condition. Thus, subdividing a basin should depend on the local extracted topographical information. As well, many studies have shown that the highest resolution data may not perform best due to the fact that the data resolution may not effectively capture the realistic hydrological processes (Lassueur *et al.* 2006). Difficulties and complexities in preparation of model input, calibration, and computational evaluation would definitely increase with promotion of data resolution. Thus, in order to improve hydrological model efficiency for a large-scale river basin, it is desirable to identify an optimal combination of DEM resolution and basin subdivision level.

Therefore, the objective of this study is to analyze the interactive effects of DEM resolutions and basin subdivision level on runoff simulation of the Kaidu River Basin, based on the semi-distributed land use-based runoff processes (SLURP) model. The SLURP model is used for dealing with spatial and temporal variations of hydrological elements and accounting for physical mechanisms of runoff yield and routing in the study basin. Different DEMs are used to examine the effect of different topographic data on the model outputs, and different basin subdivision levels are set to evaluate the uncertainty due to variation in sub-basin numbers and sizes on model performance. Multi-objective fuzzy analysis technique is also utilized to analyze the relationship among DEM resolution, basin subdivision level, and SLURP performance (i.e., Nash–Sutcliffe efficiency (*NSE*), coefficient of determination,

and deviation of volume (*DV*)). Results will help to: (1) quantify the uncertainty of input data about spatial information on model simulation, (2) disclose the interaction between DEM resolution and subdivision level, and (3) generate the optimal system inputs.

METHODOLOGY

Hydrological model

In this study, the SLURP model is selected to evaluate the impacts of DEM resolution and basin subdivision level on runoff simulation. The SLURP model is a continuous, spatially distributed, daily time step hydrological model that uses parameters associated with land cover characteristics to simulate the hydrological processes. SLURP divides a basin into a number of sub-basins which contain a number of different land covers, and consequently, each sub-basin is inner-heterogeneous and closely related to the features of land covers (Kite 2000). The vertical water balance concept is used for each land cover type within a sub-basin containing four nonlinear tanks, i.e., canopy storage, snow storage, fast storage, and slow storage, representing canopy interception, snowpack, aerated soil storage, and groundwater, respectively (as shown in Figure 1). The evapotranspiration for each land cover in each sub-basin is calculated using the Morton CRAE method:

$$E_a = \alpha E_p \tag{1}$$

where E_a is areal evapotranspiration, α is a coefficient such as the Priestley–Taylor and E_p is potential evapotranspiration. The potential evaporation can be calculated by Penman–Monteith method from the following equation:

$$E_p = \frac{D \cdot 700T_m/(100-\phi) + u(T_a - T_d)}{80 - T_a} \tag{2}$$

where $T_m = T_a + 0.006A_m$, T_a is the mean daily air temperature, A_m is the elevation (m), ϕ is the latitude in degrees, u is a wind factor, D is the number of daylight hours, and $T_a - T_d$ is the difference between air and dew point temperatures approximated by:

$$T_a - T_d = 0.0023A_m + 0.37T_a + 0.53R_m + 0.35R_{hc} - 10.9 \tag{3}$$

where R_m is the mean daily range in temperature and R_{hc} is the difference between the mean temperatures of the hottest and coldest months of the year. Snowmelt is calculated

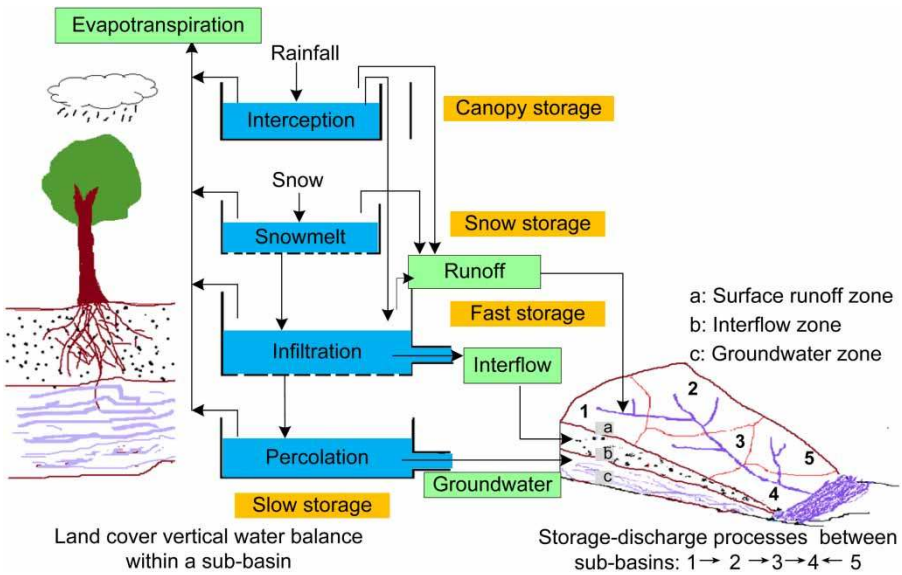

Figure 1 | Diagram of land cover vertical balance within a sub-basin and storage–discharge between sub-basins.

using the degree-day method when the temperature in degrees is above the rain/snow division temperature. Rainfall and any snowmelt infiltrates through soil surface into the fast store depending on the current infiltration rate. If precipitation factor exceeds the maximum possible infiltration rate, surface runoff is generated using the following equation:

$$Inf = \left(1 - \frac{S_1}{S_{1,\max}}\right) \cdot Inf_{\max} \tag{4}$$

$$q_s = (p - \ln f) \cdot t \tag{5}$$

where S_1 is the current contents of the rapid store, $S_{1,\max}$ is the maximum capacity of the fast store and $Inf_{\max}$ is the maximum possible infiltration rate, q_s is the surface runoff, p is the precipitation factor, and t is the delay of rainfall. The subsurface flow processes are simulated using two linear reservoirs, the fast store (an unsaturated soil layer) and the slow store (a groundwater zone). Generally, the simulation of subsurface flow processes is based on the following equations:

$$RP + RI = \frac{1}{k_1} \cdot S_1 \tag{6}$$

$$\frac{RP}{RI} = \frac{S_1/S_{1,\max}}{S_2/S_{2,\max}} \tag{7}$$

$$RG = \frac{1}{k_2} \cdot S_2 \tag{8}$$

where RP is the amount of percolation, RI is the amount of interflow, RG is the amount of groundwater flow, k_1 is the retention constant for fast store, k_2 is the retention constant for slow store, S_2 is the current contents for slow store and $S_{2,\max}$ is the maximum contents of the slow store.

Runoffs are accumulated from each land cover within a sub-basin using a time/contributing area relationship for each land cover type. To compute travel times for each land cover it is necessary to estimate velocities for travel both to-stream and down-stream. SLURP computes an average velocity (V, m^3/s) using Manning's equation:

$$V = \left(\frac{1.49}{n}\right)\theta^{2/3}\left(\frac{H}{L}\right)^{1/2} \tag{9}$$

where n is the Manning roughness of each land cover, θ is the hydraulic radius, H is the average change in elevation over the distance L to-/down-stream. The travel time to-/down-stream to the sub-basin outlet for each land cover is computed from the mean distance, the change in elevation and the stream-velocity to-/down-stream. Total travel times are the sums of the outlet of the to-stream and down-stream travel times, which are used in a linear smoothing filter to distribute the runoff from each land cover over time. The results are weighted by the percentages of the sub-basin covered by each land cover, converted to m^3/s, and added to the total flow of the sub-basin. Then, the combined runoffs route to the next sub-basin in the way of hydrological storage routing:

$$Q = \alpha R^{\beta} \tag{10}$$

where Q (m^3/s) is the outflow, R is the combined runoffs routed into the channel in the sub-basin, α and β are parameters specified to give the degrees of lag and attenuation required.

Calibration and validation

In this study, the SLURP model is calibrated and validated using two sets (i.e., 1996–2000 and 2001–2002, respectively) of continuous daily observed meteorological data and streamflow. The calibration is conducted by an automatic method using the Shuffled Complex Evaluation algorithm developed at the University of Arizona (Duan *et al.* 1992). Then, the model is validated using the values of calibrated parameters. Table 1 shows the model parameter ranges used for calibration in the Kaidu River Basin. The optimal objective functions are *NSE*, coefficient of determination (R^2), and *DV*, which are used to address the goodness-of-fit of the performance of the hydrological model. They are defined as follows:

$$\mathrm{NSE} = 1 - \frac{\sum_{i=1}^{n}\left(H_{obs,i} - H_{sim,i}\right)^2}{\sum_{i=1}^{n}\left(H_{obs,i} - \bar{H}_{obs}\right)^2} \tag{11}$$

$$R^2 = \frac{\left(n\sum_{i=1}^{n} H_{obs,i}H_{sim,i} - \sum_{i=1}^{n} H_{obs,i} \cdot \sum_{i=1}^{n} H_{sim,i}\right)^2}{\left[n\sum_{i=1}^{n} H_{obs,i}^2 - \left(\sum_{i=1}^{n} H_{obs,i}\right)^2\right]\left[n\sum_{i=1}^{n} H_{sim,i}^2 - \left(\sum_{i=1}^{n} H_{sim,i}\right)^2\right]} \tag{12}$$

Table 1 | Parameters used in calibration and assigned values for the Kaidu River Basin

Parameters	Lower bound	Upper bound	Sensitivity
Initial contents of snow store (mm)	1	1,000	Medium
Initial contents of slow store (%)	0	100	Low
Maximum infiltration rate (mm/d)	10	1,000	Low
Manning roughness (n)	0.0001	0.1	Low
Retention constant for fast store (d)	1	50	High
Maximum capacity for fast store (mm)	10	500	High
Retention constant for slow store (d)	10	500	High
Maximum capacity for slow store (mm)	100	1,000	Medium
Precipitation factor	0.8	15	High
Rain/snow division temperature (°C)	−2	0	Medium

$$DV(\%) = 100 \cdot \frac{\sum_{i=1}^{n} H_{obs,i} - \sum_{i=1}^{n} H_{sim,i}}{\sum_{i=1}^{n} H_{obs,i}} \tag{13}$$

where $H_{obs,i}$ is the observed streamflow on day i, $H_{sim,i}$ is the simulated streamflow on day i, n is the number of simulated days, and $\bar{H}_{obs}$ is the average measured streamflow.

Multi-objective fuzzy analysis

Multi-objective fuzzy analysis technique is employed to comprehensively analyze model performance and find out the most suitable combination of DEM resolution and basin subdivision level based on three optimal objectives (i.e., *NSE*, R^2, and *DV*). Fuzzy sets optimization can be extended to situations involving subjective uncertainty to ranking alternatives. An optimal choice can be considered as pattern recognition between a 'positive ideal alternative' and 'negative ideal alternative'. The value of u (closeness to the positive ideal alternative) describes the degree of acceptability from 'bad' to 'good' and varies from 0 to 1.

It is supposed that the decision matrix R consists of n alternatives (i.e., 24 scenarios) expressed as A $\{A_1, A_2 \ldots, A_n\}$ and m objectives (*NSE*, R^2, and *DV*) described by C $\{C_1, C_2 \ldots, C_m\}$. The decision matrix is represented by $V(v_{ij})_{m\times n}$, where v_{ij} is the ith objective value of alternative A_j ($j = 1, 2, \ldots, n$). In general, the objectives are classified into two types: benefit and cost. The benefit objective type means that a higher value is better while for the cost objective type the opposite is valid (Krohling & Pacheco 2015). Thus, different types of objectives can be normalized using the following formulas:

$$r_{ij} = \frac{(v_{ij} - v_{i\min})}{(v_{i\max} - v_{i\min})} \tag{14}$$

$$r_{ij} = \frac{(v_{i\max} - v_{ij})}{(v_{i\max} - v_{i\min})} \tag{15}$$

where $v_{i\max} = \vee_{j=1}^{n} v_{ij}$, $v_{i\min} = \wedge_{j=1}^{n} v_{ij}$. For the benefit type, Equation (14) should be adopted, otherwise Equation (15). After transformation, the normalized matrix can be expressed as $R(r_{ij})_{m\times n}$. For the multi-objective decision-making problem with limited alternatives, the optimal alternative is relative and thus the m positive ideal alternative is defined as: G $(g_1, g_2, \ldots, g_m)^T$ and the negative ideal alternative is defined as B $(b_1, b_2, \ldots, b_m)^T$, where $g_i = \vee_{j=1}^{n} v_{ij}$, $b_i = \wedge_{j=1}^{n} v_{ij}$, $i = 1,2, \ldots,n$. The optimal relative closeness of each alternative can be obtained by minimizing the sum of its squared distances to ranking centers. The weighted distance is used to represent the distance from G and B of each alternative, and can be respectively defined as:

$$d_j^+ = \sqrt{\sum_{i=1}^{m} [w_i(g_i - r_{ij})]^2} \tag{16}$$

$$d_j^- = \sqrt{\sum_{i=1}^{m} [w_i(r_{ij} - b_j)]^2} \tag{17}$$

In Equations (16) and (17), w is a weight vector and $w = (w_1, w_2, \ldots, w_m)^T$, $\sum_{i=1}^{m} w_i = 1$, $w_i > 0$, and $i = 1, 2, \ldots, m$. If the closeness of alternative A_j relative to G is denoted by u_j and the one relative to B is $1-u_j$, the synthetically weighted distance is given as:

$$F_j(u_j) = u_j^2 \sum_{i=1}^{m} [w_i(g_i - r_{ij})]^2 + (1 - u_j)^2 \sum_{i=1}^{m} [w_i(r_{ij} - b_i)]^2 \tag{18}$$

To obtain the optimal solution, the synthetically weighted distance is minimized: Min$\{F_j(u_j)\}$, where $j = 1, 2, \ldots,$ n. Let

$dF(u_j)/du_j = 0$, u_j can be obtained according to the following equation:

$$u_j = \frac{(d_j^-)^2}{[(d_j^+)^2 + (d_j^-)^2]} \tag{19}$$

According to the definition of relative closeness, the bigger u_j is, the better the alternative is. Thus, the relatively optimal DEM resolutions and number of sub-basins of SLURP can be obtained by ranking the closeness efficiency. A flowchart for analyzing DEM resolution and basin subdivision impacts on runoff simulation is presented in Figure 2.

STUDY AREA AND DATA

The Kaidu River Basin (42°14′N–43°21′N, 82°58′E–86°05′E) is located on the south slope of the Tianshan Mountains in Xinjiang Uyghur Autonomous Region of China. The study basin is an alpine cold-arid region with a complex topography. As shown in Figure 3, the basin has a total area of 18,827 km^2 with elevation varying from 1,400 m to 4,780 m, and the mainstream length is about 500 km. The channel density of the river basin is about 0.28 km/km^2 and the average slope is about 12.21%. The land covers in this basin include grassland (60.6%), bare land (20.9%), wetland (8.9%), snow/ice (5.1%), water (3.8%), sand (0.5%), and forest (0.2%). The average annual

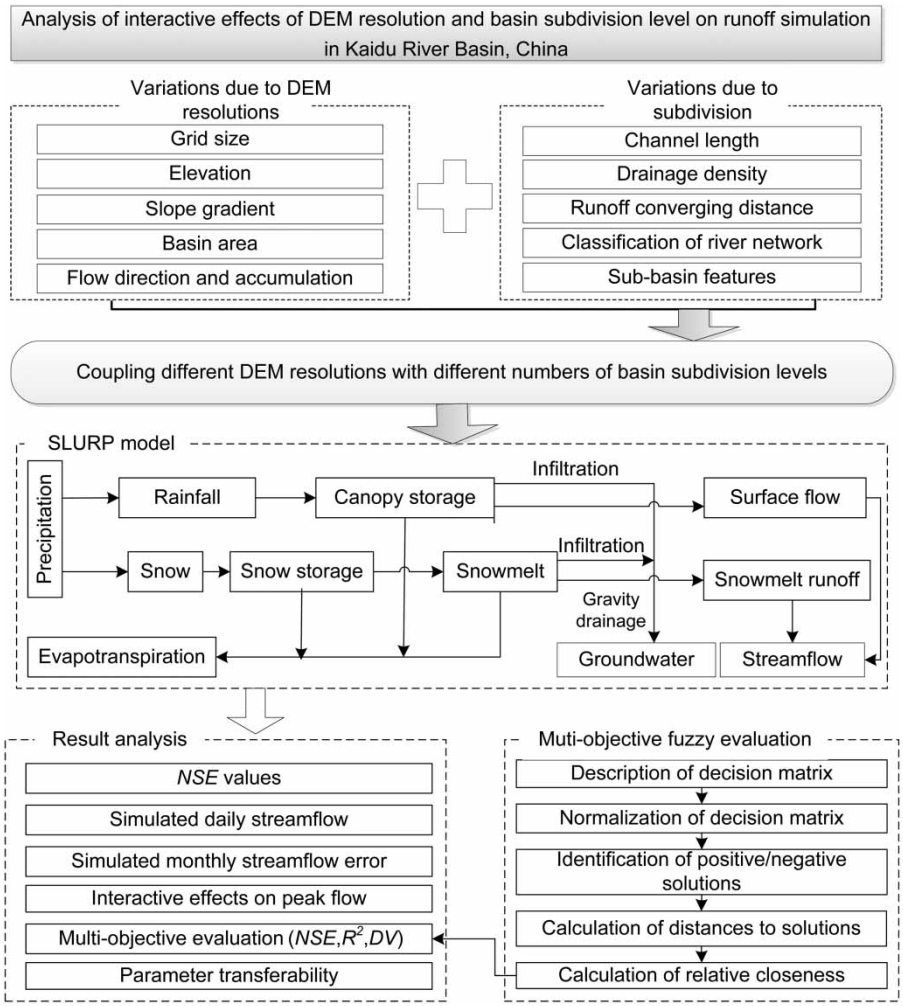

Figure 2 | Flowchart for analyzing DEM resolution and basin subdivision impacting on runoff simulation.

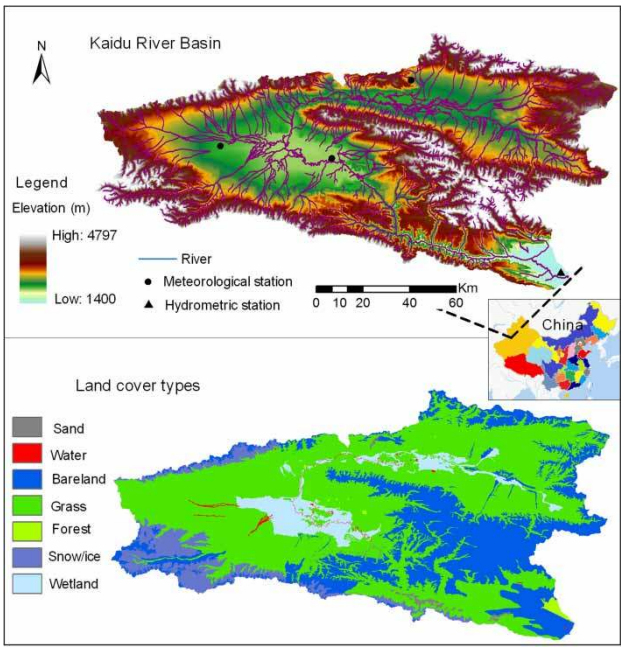

Figure 3 | Kaidu River Basin.

temperature is −4.26 °C and the minimum temperature is about −48.1 °C. It has an average annual pan evaporation of 1,100 mm and precipitation of 273 mm (Wang *et al.* 2015). The spatial and temporal distribution of temperature precipitation is uneven in this basin, and the basin is covered with snow and perennial glacier on high altitude mountains. The annual snow-cover days are as many as 139.3 days and the largest average annual snow depth is 12 cm. The hydrologic flow in the Kaidu River Basin is driven by snowmelt in the spring, rainfall/snowmelt in the summer and perennial glacier melting, which contributes to channel generation in high mountains. The importance of the river basin lies in the fact that the Kaidu River is one of the critical tributaries of the Tarim River (i.e., the largest inland river in China) and plays a role of the utmost importance in protecting the Bosten Lake. Moreover, understanding the hydrological processes, which are closely related to runoff generation and water resources volume, is critical to the sustainable development of this area. However, in the Kaidu River Basin, due to the large size and complicated topography associated with a difference of about 3,400 m in elevation, DEM resolution and basin subdivision level have important impacts on the accuracy of hydrological modeling simulation.

Spatial data used in this study include meteorological and hydrometric data, DEM, land cover type, and soil type. General meteorological data, including air temperature, precipitation, wind speed, and relative humidity, were obtained from four meteorological stations (i.e., Bayanbulak, Luotuobozi, Shenglidaoban, and Shuidianzhan) in the basin (Zhang *et al.* 2016). The streamflow data (from 1957 to 2011) for the Kaidu River were collected from Dashankou hydrometric station. The temperature input for elevation differences is derived with a lapse rate of 0.75 °C per 100 m, and precipitation data are increased by 1% per 100 m based on the data obtained from the monitoring stations following some other studies (Jing & Chen 2011; Wang *et al.* 2015). Land cover types and soil data in the year 2000 were prepared by the Resource and Environmental Sciences Data Centre Chinese Academy of Sciences (http://www.resdc.cn). Due to the data integrity and consistency with the land cover data, the period of 1996–2000 was selected to calibrate the model.

A Shuttle Radar Topography Mission 90 m DEM for the Kaidu River Basin was acquired from the Geospatial Data Cloud Website (http://www.gscloud.cn). Comprehensively based on basin size and topographic characteristics as well as model complexity, four DEMs of 150 m, 200 m, 300 m, and 500 m resolutions were adopted. As well, the nearest neighbor method was used to resample the DEM due to its accuracy and simplicity (Tan *et al.* 2015). Topographic parameterization (TOPAZ) was used to process a raster DEM into topographic and topologic variables (e.g., sub-basin areas, channel length, and distance to-/down-stream for each land cover within each sub-basin) that are physically meaningful to basin runoff processes (Lacroix *et al.* 2001). By manually specifying two parameters, the critical source area (CSA) and the minimum source channel length (MSCL), TOPAZ can delineate the channel network and segment the landscape into sub-basins at varying levels of detail. In this study, six basin subdivision levels (i.e., 15, 33, 65, 109, 183, and 285 sub-basins) were determined by TOPAZ according to different randomly generated sets of CSA and MSCL values with consideration of basin characteristics.

The basin subdivisions and main channel segments are depicted in Figure 4. As shown in Table 2, detailed basin

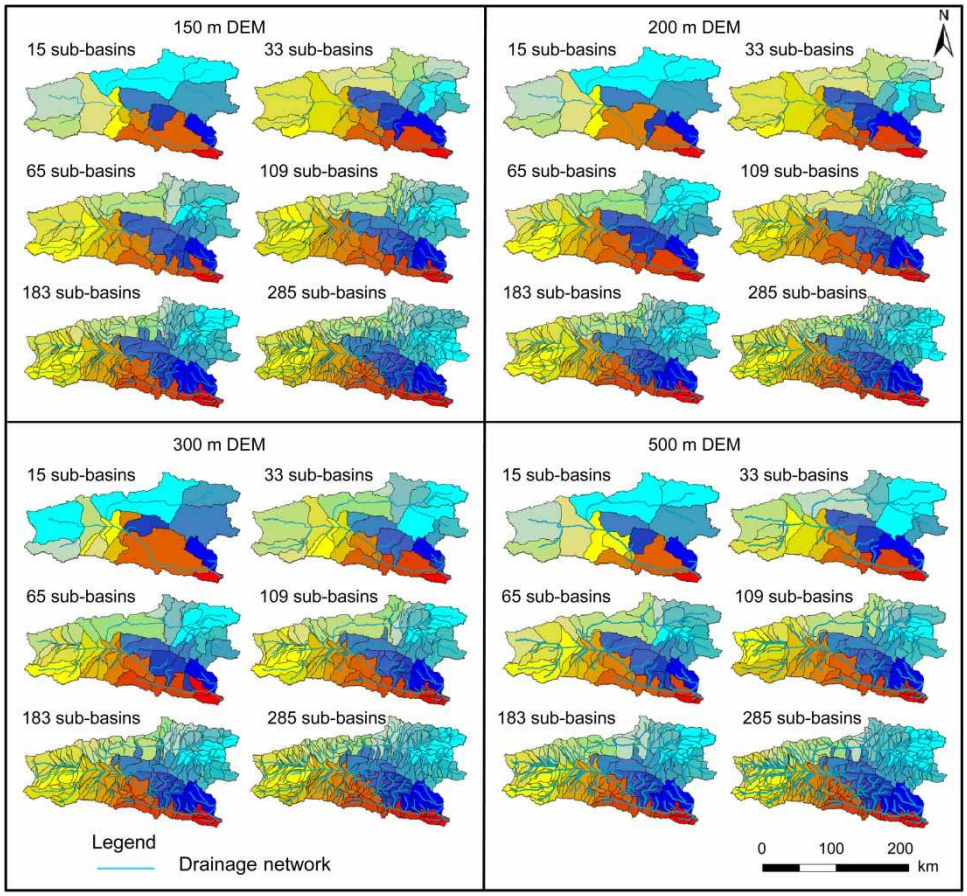

Figure 4 | Basin subdivisions and main channel segments in different scenarios (color areas represent sub-basins). Please refer to the online version of this paper to see this figure in color: http://dx.doi.org/10.2166/nh.2016.332.

subdivision would produce accurate basin elevation range; for example, under 150 m DEM, sub-basin average elevation changes from 2,380 m to 3,390 m in 15 sub-basins, but it varies from 1,720 m to 3,750 m in 285 sub-basins. However, when the basin is subdivided more finely, the minimum sub-basin area nearly approaches zero, indicating that over-detailed subdivision would contain an increased percentage of spurious sub-basins. It also revealed the channel density would increase with an increase of the number of sub-basins. For instance, under 200 m DEM, the extracted channel densities are 0.057, 0.077, 0.110, 0.157, 0.203, and 0.253 km/km^2 from 15 to 285 sub-basins, respectively. It is shown that coarse DEM resolution would result in low sub-basin slopes. For example, under 285 sub-basins, the average slopes of sub-basin are 9.68%, 9.01%, 8.24%, and 6.12% from 150 to 500 m DEM, respectively.

RESULTS AND DISCUSSION

Results of runoff simulation

In this study, 24 scenarios (i.e., 24 combinations of four resolutions and six subdivision levels) were examined to evaluate the effects of different scenarios on runoff simulation. Figure 5 depicts the observed and simulated streamflows under all scenarios. The trends of simulated streamflow are consistent with that of observed streamflow. Table 3 lists the efficiencies of model simulations. Results show that different scenarios produced changed model efficiencies. In detail, the value of *NSE* tends to increase as subdivision level increases; however, after 109 sub-basins, the increasing trend would become slight. For instance, under 200 m DEM, the values of *NSE* change only from 0.687 to 0.692 under 109 sub-basins to 285 sub-basins;

Table 2 | Key characteristics of sub-basins and model performance under different scenarios

Scenarios				Sub-basin average elevation (m)		Sub-basin area (km^2)			Slope of sub-basin (%)	
DEM	Subdivisions	CSA (ha)	MSCL (m)	Minimum	Maximum	Minimum	Maximum	Drainage density (km/km^2)	Average	Maximum
150 m	15	40,000	9,000	2,380	3,390	216	3,300	0.057	10.07	35.35
	33	22,000	6,000	2,380	3,450	16.54	2,280	0.080	11.25	41.85
	65	12,500	5,000	1,980	3,750	2.72	1,630	0.113	8.33	57.74
	109	6,000	4,000	1,980	3,750	0.14	1,210	0.163	8.41	57.74
	183	4,500	3,400	1,980	3,810	0.02	414	0.200	8.94	57.74
	285	2,600	2,900	1,720	3,900	0.02	317	0.263	9.68	57.69
200	15	38,500	9,000	2,380	3,410	56.50	3,310	0.057	10.70	39.41
	33	22,000	6,000	2,380	3,450	32.33	2,270	0.077	12.79	39.43
	65	14,000	4,500	1,980	3,760	0.04	1,630	0.110	7.91	39.43
	109	6,800	4,000	1,980	3,760	0.04	1,390	0.157	8.34	54.79
	183	4,000	3,500	1,870	3,840	0.04	501	0.203	8.38	54.79
	285	2,700	3,000	1,710	3,910	0.04	417	0.253	9.01	54.79
300	15	40,000	9,000	2,390	3,390	280	3,540	0.053	9.36	46.69
	33	20,000	6,000	2,350	3,760	2.88	2,280	0.080	11.02	48.79
	65	15,500	1,500	2,350	3,760	2.88	1,890	0.097	7.73	48.79
	109	6,500	3,800	2,070	3,760	1.08	1,450	0.153	7.52	48.79
	183	4,000	3,500	2,000	3,760	1.08	452	0.200	8.12	48.79
	285	2,700	3,000	1,720	3,810	0.09	291	0.247	8.24	48.79
500	15	41,000	9,000	2,420	3,390	102	3,140	0.050	9.08	26.05
	33	22,000	6,000	2,420	3,440	11.51	1,860	0.073	9.95	27.92
	65	12,000	5,000	2,000	3,750	5.52	1,570	0.113	7.57	38.67
	109	6,450	4,300	2,050	3,750	0.25	1,410	0.147	5.96	38.67
	183	4,000	3,500	1,720	3,820	0.25	465	0.197	6.03	38.67
	285	2,700	3,000	1,720	3,900	0.25	284	0.240	6.12	38.67

CSA, critical source area.
MSCL, minimum source channel length.

however, the values of *NSE* change from 0.561 to 0.671 under 15 sub-basins to 65 sub-basins. Also, as shown in Figure 6, the fitting results between observed and simulated streamflows during calibration and validation periods further validate that increasing subdivision levels could improve the model performance. This is due to the fact that finer subdivision levels would preserve the more natural flow paths, boundaries and channels, providing more detailed and accurate input information. When the number of sub-basins is more than 109, the slight increase of *NSE* value is due to the increased spurious area that the hydrological model could not identify; the obtained results have a consistent tendency with the results of Rouhani *et al.* (2009) and Han *et al.* (2014).

Moreover, results also show that an optimum DEM resolution exists for hydrological model applications. In detail, 200 m DEM resolution produces better model efficiency compared to other resolutions. However, the *NSE* values obtained under 150 m DEM resolution are slightly less than those under 200 m DEM. For example, under 285 sub-basins, the *NSE* values are 0.677 and 0.692 under 150 m and 200 m DEM, respectively. The streamflow fitting results further reveal that the simulated streamflow under 200 m DEM are closer to observed ones (as shown in Figure 7). This can be attributed to the fact that more grids and input information are produced under 150 m DEM; there are more cumulative sampling errors and more obvious faults in higher resolutions of DEM which can be eliminated when resampled to proper low resolutions due to the elimination of the amount of sampling points and increase of grid size. On the other hand, the DEM-based hydrological model is established on the assumption that the local river slope is equal to the local terrain gradient, which may not fit well with the realistic river slope. Besides,

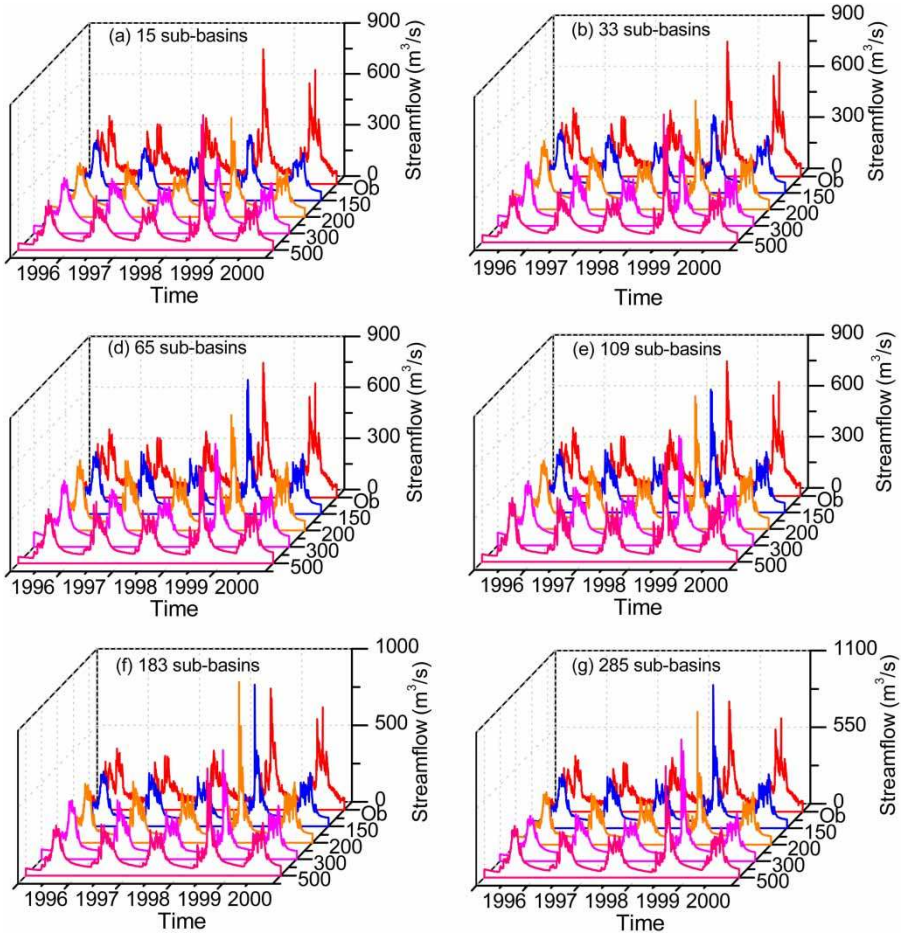

Figure 5 | Simulated and observed streamflows during calibration period (Ob represents the observed streamflow).

when the DEM resolution is coarser than 200 m, *NSE* values decrease due to the fact that lower resolution reduces the variation in altitude and slopes. Therefore, appropriate DEM should be balanced before model preparation in order to obtain the best model efficiency and save operating time.

Furthermore, results also demonstrate that in coarse subdivision levels, the *NSE* values would have a negligible variation with the change of DEM resolutions. For instance, when the basin is subdivided into 15 sub-basins, the *NSE* values are around 0.550 with a fluctuation of 4% of the minimum value (i.e., 0.543). It is indicated that in 15 sub-basins, the effect of DEM resolutions can be neglected during the calibration processes. Among all scenarios, the combination of 200 m DEM and 285 sub-basins produces the best model performance. The *NSE* values are 0.692 (in the calibration period) and 0.60 (in the validation period); the *DV*s (%) are 10.70 and 6.22 respectively; the values of R^2 for calibration and validation are 0.72 and 0.60, respectively, indicating a good consistency between observed streamflow and simulated streamflow. Compared with the value of *NSE* (i.e., 0.65) acquired in Wang *et al.* (2015), the obtained results further indicated that high DEM resolution is not always necessary in Kaidu River Basin for pursuing the optimal combination of DEM resolution and subdivision level.

Figure 8 presents the monthly simulated streamflow error (i.e., average monthly simulated streamflow minus monthly observed streamflow) in the calibration period (1996–2000) and validation period (2001–2002), respectively. Results show that a higher streamflow error occurs during April, May, and June than the other months. This is mainly because the streamflow in those 3 months is

Table 3 | Daily time series hydrological simulation results

Scenarios		*NSE*		R^2		*DV* (%)	
DEM	**Subdivision**	**C**	**V**	**C**	**V**	**C**	**V**
150	15	0.566	0.538	0.62	0.54	16.64	11.38
	33	0.625	0.569	0.65	0.53	9.94	3.83
	65	0.657	0.586	0.72	0.53	16.88	11.48
	109	0.669	0.597	0.72	0.53	13.24	9.87
	183	0.673	0.598	0.72	0.54	15.22	4.93
	285	0.677	0.588	0.72	0.55	15.38	8.67
200	15	0.561	0.547	0.63	0.57	17.76	10.97
	33	0.622	0.563	0.65	0.56	10.01	8.65
	65	0.671	0.586	0.72	0.56	10.32	9.77
	109	0.687	0.602	0.70	0.59	10.53	9.02
	183	0.690	0.597	0.73	0.57	9.46	5.30
	285	0.692	0.600	0.72	0.60	10.70	8.22
300	15	0.549	0.524	0.59	0.56	13.62	12.19
	33	0.587	0.550	0.67	0.53	12.38	7.86
	65	0.631	0.567	0.65	0.56	7.18	9.38
	109	0.646	0.573	0.66	0.56	7.00	9.58
	183	0.651	0.585	0.69	0.56	8.89	2.71
	285	0.655	0.577	0.68	0.57	10.42	6.10
500	15	0.543	0.461	0.64	0.55	20.76	10.66
	33	0.587	0.489	0.67	0.55	19.35	12.30
	65	0.613	0.516	0.66	0.56	12.11	11.03
	109	0.628	0.537	0.69	0.52	12.07	10.89
	183	0.634	0.535	0.66	0.56	11.17	8.12
	285	0.642	0.542	0.67	0.56	10.32	6.20

C, calibration period.
V, validation period.

contributed to by both snowmelt and rainfall. Figure 8(a) reveals that 200 m DEM resolution would produce the best matched simulated streamflow to the observed streamflow, further implying that the model output would be promoted by the appropriate DEMs as they could provide more realistic input. Figure 8(b) shows that coarse subdivision levels have a higher streamflow error than fine ones. This is because coarse subdivision levels lead to a reduction of drainage density and simplification of channel description, which can decrease the accuracy of runoff simulations. The obtained results suggest providing a scientific support for decision-makers to decide which scenario is suitable for seasonal water resources management.

Figure 9 depicts the interactive effects of DEM resolution and basin subdivision level on the simulated peak flow. Results show that the estimated peak flow fluctuation among the six subdivision levels is larger under high DEM resolutions than under low ones. Similarly, the fluctuation among the four DEM resolutions is larger under fine subdivision levels than under coarser ones. For example, in Figure 9(a), under 500 m DEM, the peak flow would change from 557 m^3/s to 701 m^3/s with a standard deviation of 52 m^3/s; under 150 m DEM, the peak flow would range from 482 m^3/s to 1,014 m^3/s with a standard deviation of 190 m^3/s. The result indicates that basin subdivision does not almost necessarily influence peak flow, especially under low DEM resolution. This is because low DEM resolution would smooth the topography, and the difference in river characteristics among all subdivision levels is smaller than that in high DEM resolutions. The results indicate that an interactive effect exists between DEM resolution and subdivision level. Figure 9(b) visualizes that under 33 sub-basins, the range of peak flow would change from 530 m^3/s to 677 m^3/s with a standard deviation of 64 m^3/s; under 183 sub-basins, the peak flow would range from 557 m^3/s to 1,014 m^3/s with a standard deviation of

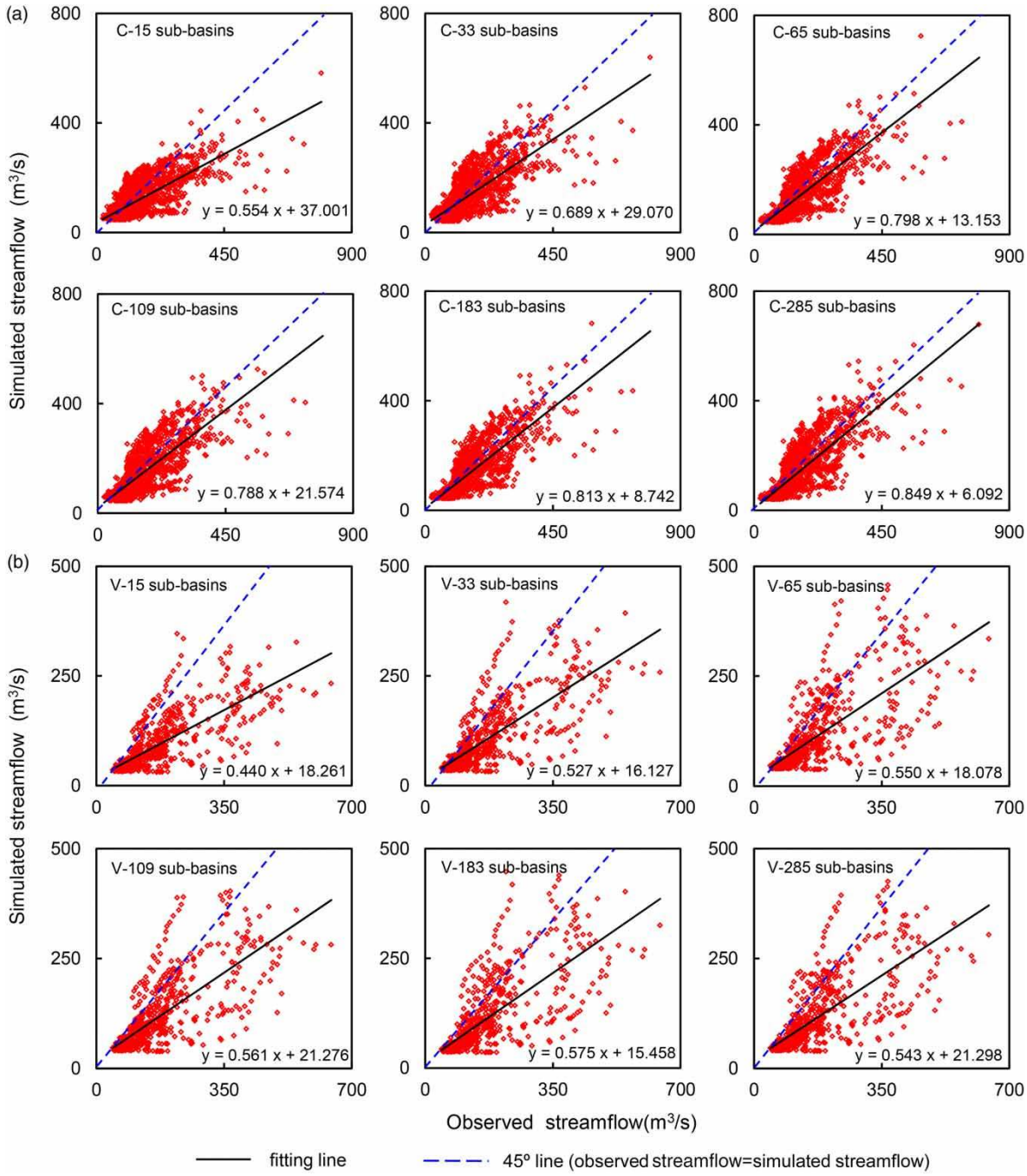

Figure 6 | Scatter plots of observed and simulated discharges during (a) calibration and (b) validation period under 200 m DEM.

212 m^3/s. This is because less dense drainage and less accumulative errors derived from DEM resampling in coarse subdivision levels could lead to slighter differences in peak flow. Results also show that the peak flow increases with increased number of sub-basins. This is due to the fact that increasing basin subdivision level results in increment of the total length of channels, as well as a reduction in overland flows. However, further increment in drainage density does not cause a significant change in peak runoff at the basin outlet. Merits and demerits should be balanced to

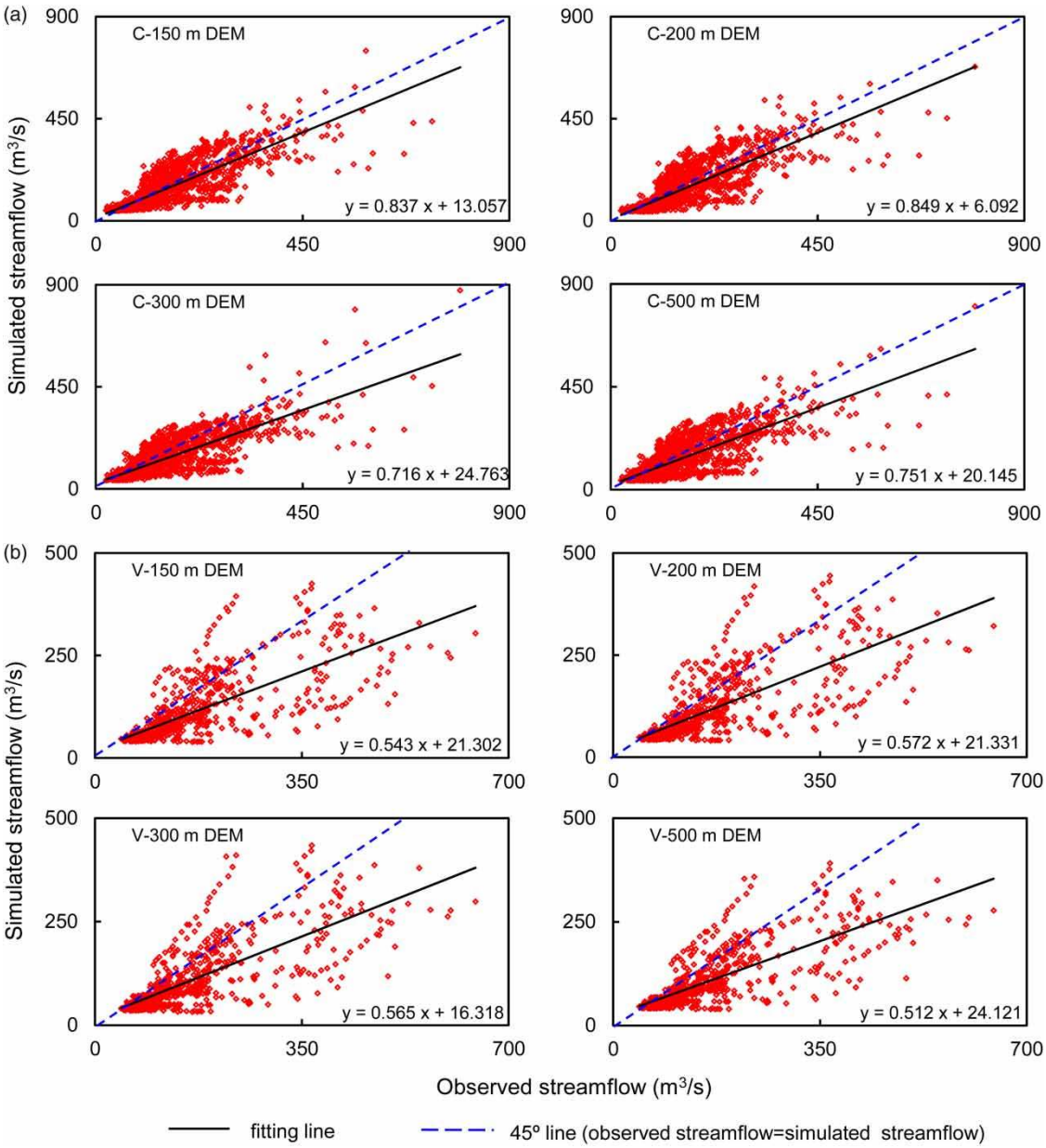

Figure 7 | Scatter plots of observed and simulated discharges during (a) calibration and (b) validation period under 285 sub-basins.

choose the optimum scenario before decision-making related to flood controlling.

Comparison of parameter transferability

Runoff generation processes are sensitive to the sub-basin size and topographic slope, variation in runoff yielding, and flow routing parameters are needed in all scenarios. Twenty-four scenarios have been calibrated respectively to pursue the optimal runoff simulation results. Results show that some parameters have a slight difference among different scenarios. For example, the maximum retention constant for grassland changes in a deviation of 8% compared to the minimum value (i.e., 72.3 mm). This is due to the fact that several parameters are determined based on soil and land types rather than drainage network and sub-basin relief. However,

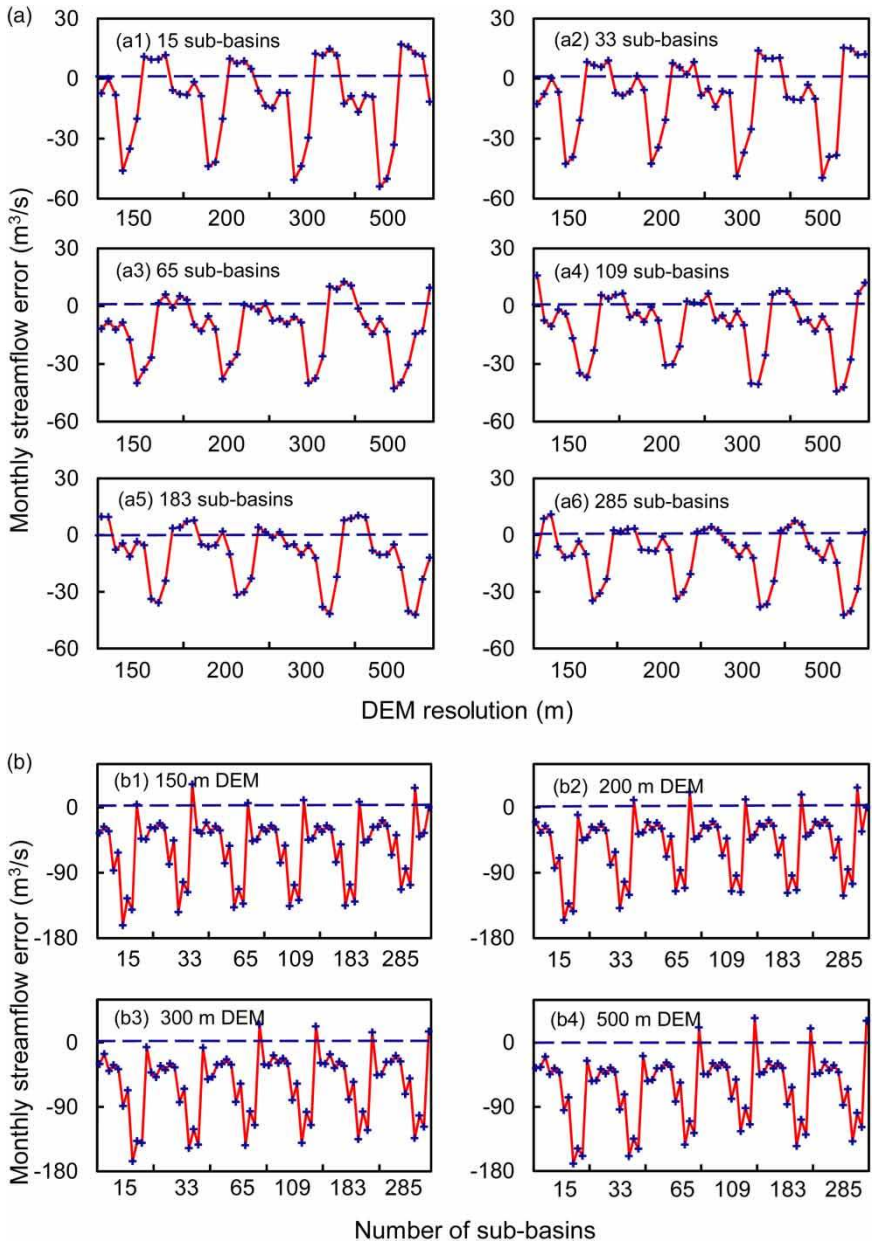

Figure 8 | Average monthly simulated streamflow errors (simulated streamflow minus observed streamflow) during (a) calibration and (b) validation period.

to explore whether the parameters under one scenario are suitable for the others without calibration requires parameter transferability. After transferring the parameters in the period of 1996–2002 among different scenarios, results show that the range of the values of *NSE* is wider under parameter transferability among different subdivision levels (i.e., from 0.411 to 0.640) than that among different DEM resolutions (i.e., from 0.421 to 0.602). The obtained results suggest that the uncertainty due to subdivision levels should give rise to more attention to hydrological simulation. Moreover, Figure 10(a) indicates that parameter transferability has less variable effects on the modeling performance under 500 m DEM compared to other DEM resolutions. In detail, when the subdivision is greater than 65 sub-basins, all the *NSE* values change from 0.462 to 0.551 under 500 m DEM resolution; however, the *NSE* values would change from 0.452

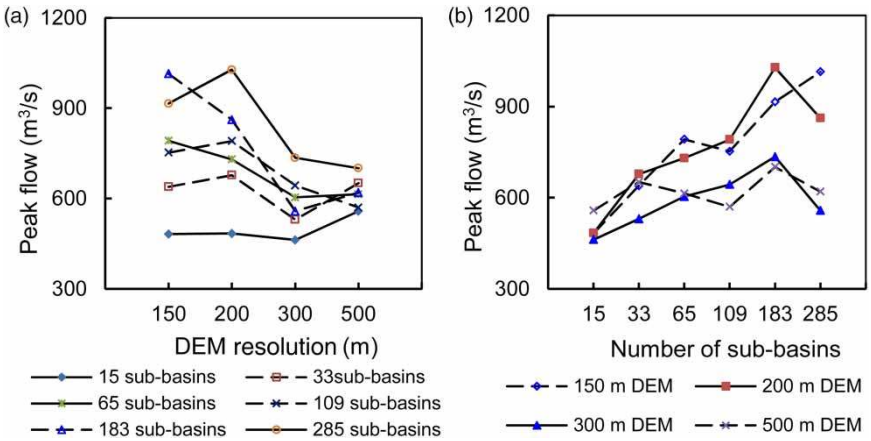

Figure 9 | Interaction plot for simulated peak flow (m^3/s) in calibration period (1996–2000).

to 0.615 under 150 m DEM resolution. Correspondingly, it seems not necessary to calibrate and optimize parameters for each subdivision, especially for fine subdivision levels under 500 m DEM resolution. Similarly, in Figure 10(b), under15 sub-basins, the variation in *NSE* values derived from transferability among the four DEM resolutions is smaller than that in other scenarios. The results indicate that in coarse subdivision levels, the parameters obtained in all DEM resolutions can be interchangeable without further calibration. Results also show that parameters derived from fine subdivision levels or high DEM resolutions might not perform well for coarse subdivision levels or low DEM resolutions. Generally, the analysis of parameter transferability provides a reference for decision-makers to decide whether the obtained parameters could be used in future model operation in the Kaidu River Basin.

Uncertainty analysis for model efficiencies

However, the above analyses only focus on one kind of result to assess the impacts of DEM resolution and basin subdivision level, which would amplify the uncertainties in model performance assessment. In order to mitigate such uncertainty and to select the best fitted DEM resolution and basin subdivision level, a multi-objective fuzzy evaluation method which integrates multi-results (i.e., *NSE*, R^2, and *DV*) is adopted. *NSE*, R^2, and *DV* are three indices for representing SLURP efficiency with a weighted vector of $w = (1/3, 1/3, 1/3)$. The high values of *NSE* and R^2 represent the high efficiency of the model, and *DV* the opposite. Thus, the objectives of *NSE* and R^2 were normalized using the benefit type, and the objective of *DV* was normalized using the cost benefit. The relative closeness of different scenarios both in the calibration and validation period are obtained by multi-objective fuzzy evaluation method (shown in Figure 11). Results show that 15 sub-basins have the lowest closeness (i.e., the worst model performance) both in the calibration and validation period. For example, the closeness is 0.050 under 500 m DEM and 15 sub-basins in calibration, revealing that 500 m DEM and 15 sub-basins is the worst selection for model simulation. Among all the scenarios, 200 m DEM resolution coupled with 183 sub-basins has the highest closeness (i.e., 0.988 and 0.896, respectively) both in the calibration and validation period, which is different from the result only using *NSE*. The reason for this is that R^2 and *DV* possess the same important role compared with *NSE*, however, in this study, R^2 and *DV* do not show an obvious trend like *NSE*, and thus the integrated evaluation is different. However, the results further validate that over-detailed basin subdivision would not always promote the model performance.

CONCLUSIONS

This study has investigated the interactive effects of DEM resolution and subdivision level on runoff simulation of Kaidu River Basin, using the SLURP model. Results show

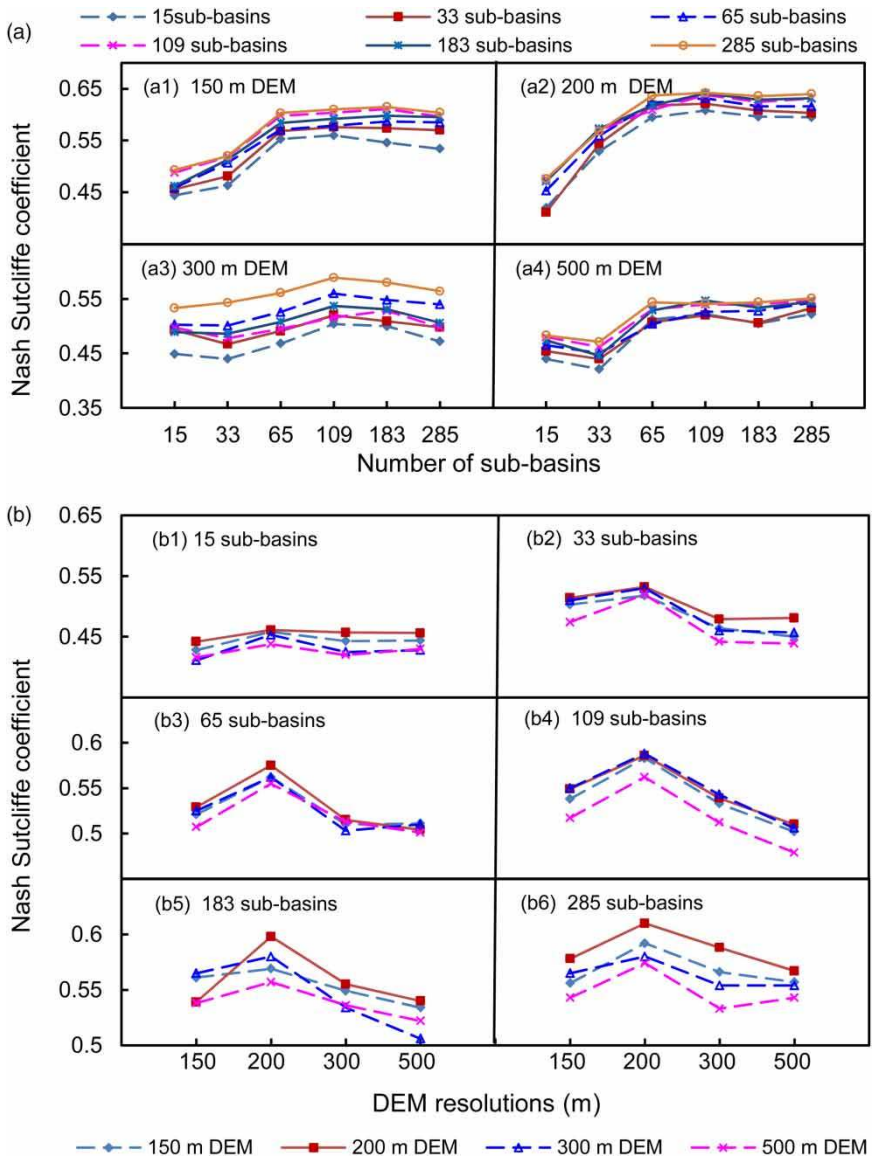

Figure 10 | Model transferability performances between different (a) subdivision levels and (b) DEM resolutions in the period 1996–2002 under all scenarios.

that with the increasing number of sub-basins, the value of *NSE* and peak flow would increase, and the monthly streamflow error would decrease. However, after 109 sub-basins, the increasing/decreasing trend becomes slight. For DEM resolution, it is under 200 m DEM (not the highest resolution) that the model has better simulation results than those under others. Multi-objective fuzzy evaluation suggests that at 200 m DEM and 183 sub-basins, the simulation result is better than that at other scenarios, suggesting that over-detailed sub-basins may not necessarily promote model performance. Moreover, the results of peak flows indicate that high DEM resolutions in coarse subdivision levels or fine subdivision levels in low DEM resolutions are not necessary. Parameter transferability indicates that subdivision level has a more obvious effect on the model efficiency than DEM resolution and more attention should be paid to uncertainties derived from basin subdivision levels during the model preparation. The obtained results will help to provide evidence of the scientific validities of the model, generate the optimal system inputs, as well as

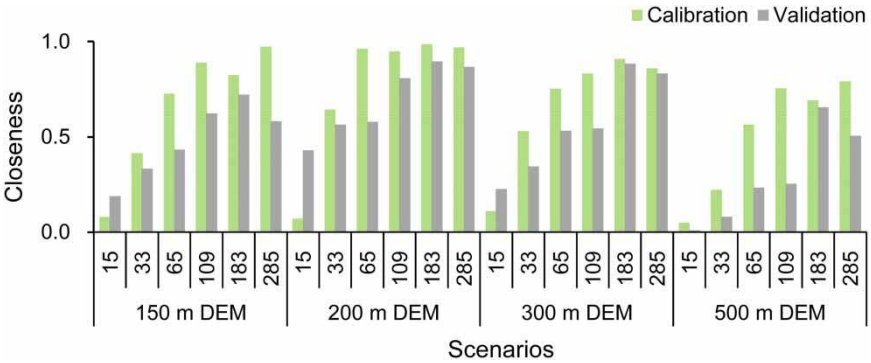

Figure 11 | The relative closeness of different scenarios.

provide the basis for predicting the effects of future exogenous factors and policy choices.

However, high DEM resolutions and over-detailed subdivisions are time-consuming and memory-intensive in the model input preparation and complicated in the model operation. Therefore, there is a need to weigh merits and demerits before selecting the input type depending on the basin size, basin topographic feature, compute efficiency expected, as well as the level of accuracy required. Furthermore, due to the complexes in model structure, model parameters and daily input data also should be considered. It will also be interesting to explore the effects of numbers and size of raster grids on model performance in future research works. As well, it is desirable to conduct investigations into the effects of DEM resolutions and basin subdivisions for other hydrological models (e.g., SWAT).

ACKNOWLEDGEMENTS

This research was supported by the National Key Research Development Program of China (2016YFC0502803 and 2016YFA0601502), and National Natural Sciences Foundation (51379075 and 51225904), and the Fundamental Research Funds for the Central Universities (2016XS90). The authors are grateful to the editors and the anonymous reviewers for their insightful comments and suggestions.

REFERENCES

Blanchard, S. D., Pontius Jr, R. G. & Urban, K. M. 2015 Implications of using 2 m versus 30 m spatial resolution data for suburban residential land change modeling. *Journal of Environmental Informatics* **25** (1), 1–13.

Du, J. K., Xie, H., Hu, Y. J., Xu, Y. P. & Xu, C. Y. 2009 Development and testing of a new storm runoff routing approach based on time variant spatially distributed travel time method. *Journal of Hydrology* **369**, 44–54.

Duan, Q., Sorooshian, S. & Gupta, V. 1992 Effective and efficient global optimization for conceptual rainfall-runoff models. *Water Resources* **28** (4), 1015–1031.

Han, J. C., Huang, G. H., Zhang, H., Li, Z. & Li, Y. P. 2014 Effects of watershed subdivision on semi-distributed hydrological simulations: case study of the SLURP model applied to the Xiangxi River watershed. *Hydrological Sciences Journal* **59** (1), 108–125.

Jing, L. & Chen, B. 2011 Hydrological modeling of subartic wetlands: comparison between SLURP and WATFLOOD. *Environmental Engineering Science* **28** (7), 521–533.

Kalin, L., Govindaraju, R. S. & Hantush, M. M. 2003 Effect of geomorphologic resolution on modeling of runoff hydrograph and sedimentograph over small watersheds. *Journal of Hydrology* **276**, 89–111.

Kite, G. 2000 Using a basin-scale hydrological model to estimate crop transpiration and soil evaporation. *Journal of Hydrology* **229**, 59–69.

Krohling, R. A. & Pacheco, A. G. C. 2015 A-TOPSIS – an approach based on TOPSIS for ranking evolutionary algorithms. *Procedia Computer Sciences* **55**, 308–317.

Lacroix, M. P., Martz, L. W., Kite, G. W. & Garbrecht, J. 2001 Using digital terrain analysis modeling techniques for the parameterization of a hydrologic model. *Environmental Modelling and Software* **17** (2), 125–134.

Lassueur, T., Joost, S. & Randin, C. F. 2006 Very high resolution digital elevation models: do they improve models of plant species distribution. *Ecological Modelling* **198** (1–2), 139–153.

Li, L. & Xu, C. Y. 2014 The comparison of sensitivity analysis of hydrological uncertainty estimates by GLUE and Bayesian method under the impact of precipitation errors. *Stochastic Environment Research and Risk Assessment* **28**, 491–504.

Li, H., Beldring, S. & Xu, C. Y. 2014 Implementation and testing of routing algorithms in the distributed HBV model for mountainous catchments. *Hydrology Research* **45** (3), 322–333.

Ma, G. 2014 Flow velocity and travel time determination on rid basis using spatially varied hydraulic radius. *Journal of Environmental Informatics* **23** (2), 36–46.

Pradhanang, S. M. & Briggs, R. D. 2014 Effects of critical source area on sediment yield and streamflow. *Water and Environment Journal* **28**, 222–232.

Rouhani, H., Willems, P. & Feyen, J. 2009 Effect of watershed delineation and areal rainfall distribution on runoff prediction using the SWAT model. *Hydrology Research* **40** (6), 505–519.

Singh, V., Goyal, M. K. & Chu, X. 2015 Multicriteria evaluation approach for assessing parametric uncertainty during extreme peak and low flow conditions over snow glaciated and inland catchments. *Journal of Hydrologic Engineering* **21** (1), 04015044.

Tan, M. L., Ficklin, D. L., Dixon, B., Ibrahim, A. L., Yusop, Z. & Chaplot, V. 2015 Impacts of DEM resolution, source, and resampling technique on SWAT-simulated streamflow. *Applied Geography* **63**, 357–368.

Tripathi, M. P., Raghuwanshi, N. S. & Rao, G. P. 2006 Effect of watershed subdivision on simulation of water balance components. *Hydrological Processes* **20** (5), 1137–1156.

Wang, C. X., Li, Y. P., Zhang, J. L. & Huang, G. H. 2015 Assessing parameter uncertainty in semi-distributed hydrological model based on type-2 fuzzy analysis – a case study of Kaidu River Basin. *Hydrology Research* **46** (6), 969–983.

Wu, S., Li, J. & Huang, G. H. 2007 Modelling the effects of elevation data resolution on the performance of topography-based watershed runoff simulation. *Environmental Modelling and Software* **22** (9), 1250–1260.

Xu, C. Y. 1999 Operational testing of a water balance model for predicting climate change impacts. *Agricultural and Forest Meteorology* **98–99**, 295–304.

Xu, C. Y. & Singh, V. P. 2004 Review on regional water resources assessment models under stationary and changing climate. *Water Resources Management* **18**, 591–612.

Yan, C. G. & Zhang, W. C. 2014 Effects of model segmentation approach on the performance and parameters of the Hydrological Simulation Program – Fortran (HSPF) models. *Hydrology Research* **45** (6), 893–907.

Yu, Z. 1997 Grid-spacing effect on watershed hydrologic simulations. *Hydrological Science and Technology* **13** (1–4), 75–85.

Zhang, P. P., Liu, R. M., Bao, Y. M., Wang, J. W., Yu, W. W. & Shen, Z. Y. 2014 Uncertainty of SWAT model at different DEM resolutions in a large mountainous watershed. *Water Research* **53**, 132–144.

Zhang, J. L., Li, Y. P., Huang, G. H., Chen, X. & Bao, A. M. 2016 Assessment of parameter uncertainty in hydrological model using a Markov-Chain-Monte-Carlo-based multilevel-factorial-analysis method. *Journal of Hydrology* **538**, 471–486.

First received 30 April 2016; accepted in revised form 24 June 2016. Available online 8 August 2016